Journal of Biomolecular NMR (2019) 73:477–491
https://doi.org/10.1007/s10858-019-00256-2

ARTICLE

Partial alignment, residual dipolar couplings and molecular symmetry in solution NMR

Justin L. Lorieau[1]

Received: 14 January 2019 / Accepted: 6 June 2019 / Published online: 12 August 2019

Abstract

Residual dipolar couplings (RDCs) and residual anisotropic chemical shifts (RACSs) are produced by the partial alignment of solution NMR samples. RDCs and RACSs yield high-resolution structural and dynamic information on the orientation of bonds and chemical groups in molecules. Many molecules form oligomers or have intrinsic symmetries, which may simplify the analysis of their partial alignment datasets. In this report, we explore the theory of partial alignment using an irreducible spherical representation, and we investigate the impact of molecular symmetry on the alignment of molecules. Though previous studies have reported simplified relationships on the partial alignment of molecules bearing different symmetry groups, we show that these simplified relationships may not be universal and only apply to a limited set of systems.

Keywords Wigner rotation · RDC · Oligomer

Introduction

Magnetic dipole–dipole (dipolar) couplings and the anisotropic contribution to chemical shifts contain rich information on nuclear spins in molecules. In solution NMR, these interactions can be measured through their relaxation contribution from the second order rotating frame (RF) Hamiltonian (Goldman 1988). However, molecules rotate isotropically, and these interactions typically do not contribute directly to a spectrum and the first order RF Hamiltonian.

Partial alignment with liquid crystals, distorted gels or paramagnetic tags bias the rotational diffusion of molecules to a slightly anisotropic distribution, thereby introducing residual dipolar couplings (RDCs) and residual anisotropic chemical shifts (RACSs) in the spectrum (Saupe 1968; Tolman et al. 1995; Tjandra and Bax 1997; Tycko et al. 2000; Cornilescu and Bax 2000).[1] RDCs and RACSs are useful in accurately defining the orientation of bonds in molecules and the dynamics of spins on a sub-microsecond to sub-millisecond timescale (Bax 2003; Blackledge 2005).

The analysis of RDCs and RACSs involves the identification of a partial alignment frame defined by 5 or fewer components of a Saupe matrix Losonczi et al. (1999). The orientation of bonds from RDCs and chemical shift tensors from RACS can be used to refine the structures of molecules to high accuracy. However, it is unclear how molecular symmetry, with homodimers, homotrimers or higher order oligomers, might impact the alignment frame tensor or how the orientation of the overall molecule with respect to the alignment frame might contain useful information. Previous reports describe simple relationships for the alignment tensor of RDC datasets. For example, homotrimers with a C_3 axis of symmetry are described to have axially symmetric alignment tensors (Bolon et al. 1999; Al-Hashimi et al. 2000; Saupe 1968)—i.e. the rhombicity of the alignment tensor, R_h, is equal to 0.

In this article, we explore the theory of partial alignment for a more complete set of molecular symmetries using an irreducible spherical representation. The results of this approach are analogous to results from Dennis Torchia and others in which n-site hops, or n-site exchanges, average and reshape

Electronic supplementary material The online version of this article (doi:https://doi.org/10.1007/s10858-019-00256-2) contains supplementary material, which is available to authorized users.

✉ Justin L. Lorieau
justin@lorieau.com

[1] Department of Chemistry, University of Illinois at Chicago, 4500 SES, 845 W Taylor St, Chicago, IL 60607, USA

[1] We have elected to use the RACS, instead of the more commonly used residual chemical shift anisotropy (RCSA), because partial alignment does not directly report on the anisotropy of the chemical shift.

quadrupolar tensors in the solid-state (Batchelder et al. 1983; Sarkar et al. 1986; Mack and Torchia 1991). In this case, we use a series of n-site exchanges to model the average alignment tensor for a biomolecule. We are able to reproduce the simple alignment tensor equations described in previous reports, yet we argue that these relationships hold only for a subset of alignment circumstances. We show that the alignment tensor asymmetry and molecular orientation cannot be reliably used to make conclusions on the oligomeric state or axis of rotation for a molecule.

Background

The problem

The subtleties of RDCs for homo-oligomers can be illustrated with a homotetrameric protein with a C_4 axis of rotation. According to previous approaches, the alignment tensor for a homotetramer, like a homotrimer, should be axially symmetric (i.e. $R_h = 0$) Saupe (1968).

Figure 1 shows 2 different sets of RDCs and interaction (alignment) orientations for a homotetramer with a single bond per subunit. The coordinate system (x/y/z) drawn in the background represents the fixed coordinate system of the alignment medium or laboratory frame. It is independent of the molecule.

In RDC set 1, the C_4 axis of the tetramer is aligned along the z-axis relative to the external frame. The bond (m_1) is oriented along the y-axis, and its corresponding bonds in the other subunits, m_2, m_3 and m_4, are oriented along the -x, -y and x axes, respectively.

The RDCs for alignment 1 are presented in RDC set 1 with a $D_a = 10.0$ Hz and $R_h = 0.0$. All 4 bonds have a polar angle (θ) of 90° relative to the fixed frame. They differ in their azimuthal angles (ϕ). We calculate the RDCs for the bonds using the RDC equation.

$$D(\theta_j, \phi_j) = D_a\left\{\tfrac{1}{2}\left(3\cos^2\theta_j - 1\right) + \tfrac{3}{4}R_h \sin^2\theta_j \cos 2\phi_j\right\} \tag{1}$$

The RDC for all bonds is −5.0 Hz.

$$\begin{aligned} D_{m1} &= (10.0\text{ Hz})\left\{\tfrac{1}{2}\left(3\cos^2 90° - 1\right)\right\} \\ &= -5.0\text{ Hz} \\ &= D_{m2} = D_{m3} = D_{m4} \end{aligned} \tag{2}$$

Since all 4 bonds exchange rapidly by rotation of the C_4 axis, they have the same average RDC of −5.0 Hz. Furthermore, if rotation about the C_4 axis is more rapid than the evolution time scale of chemical shifts (milliseconds), then only 1 peak is measured for all 4 bonds.

RDC set 2 shows the same molecule with its C_4 axis rotated 45° about the y-axis with the rotation matrix $\mathbf{R_y}(\mathbf{45°})$. 2 of the 4 bonds adopt new polar angles relative to the fixed frame, producing bonds n_2 and n_4, and the other 2 bonds remain unchanged (n_1 and n_3).

Again the $D_a = 10.0$ Hz and $R_h = 0.0$. The RDCs for each bond is calculated with Eq. (1) and the polar and azimuthal angles relative to the fixed frame.

$$\begin{aligned} D_{n1} &= (10.0\text{ Hz})\left\{\tfrac{1}{2}\left(3\cos^2 90° - 1\right)\right\} = -5.0\text{ Hz} \\ D_{n2} &= (10.0\text{ Hz})\left\{\tfrac{1}{2}\left(3\cos^2 45° - 1\right)\right\} = 2.5\text{ Hz} \\ D_{n3} &= (10.0\text{ Hz})\left\{\tfrac{1}{2}\left(3\cos^2 90° - 1\right)\right\} = -5.0\text{ Hz} \\ D_{n4} &= (10.0\text{ Hz})\left\{\tfrac{1}{2}\left(3\cos^2 135° - 1\right)\right\} = 2.5\text{ Hz} \end{aligned} \tag{3}$$

The 4 bonds rotate about the C_4 axis and produce an average value of −1.25 Hz.

$$\begin{aligned} D_{ave} &= (-5.0\text{ Hz} + 2.5\text{ Hz} - 5.0\text{ Hz} + 2.5\text{ Hz})/4 \\ &= -1.25\text{ Hz} \end{aligned} \tag{4}$$

The challenge in the analysis of homo-oligomers arises when the molecule may align and average between multiple orientations to produce an averaged set of RDCs. In this example, the homotetramer exchanges equally between the interaction orientations from RDC set 1 and RDC set 2 to create a new set of averaged RDCs.

$$\begin{aligned} D_{w1} &= (-5.0\text{ Hz} - 5.0\text{ Hz})/2 = -5.0\text{ Hz} \\ D_{w2} &= (-5.0\text{ Hz} + 2.5\text{ Hz})/2 = -1.25\text{ Hz} \\ D_{w3} &= (-5.0\text{ Hz} - 5.0\text{ Hz})/2 = -5.0\text{ Hz} \\ D_{w4} &= (-5.0\text{ Hz} + 2.5\text{ Hz})/2 = -1.25\text{ Hz} \\ D_{ave} &= (-5.0\text{ Hz} - 1.25\text{ Hz} - 5.0\text{ Hz} - 1.25\text{ Hz})/4 \\ &= -3.125\text{ Hz} \end{aligned} \tag{5}$$

The new average structure has bonds w_1, w_2, w_3 and w_4. The new averaged vectors for bonds w_2 and w_4 are between the vectors for bonds m_2/n_2 and m_4/n_4, respectively. The bond vectors w_1 and w_3 have the same orientation as bonds m_1/n_1 and m_3/n_3, respectively.

How are these RDCs modeled together? If we choose an average bond orientation with a θ angle of 90° and use an axially symmetric alignment tensor ($R_h = 0$), a D_a of 6.25 Hz could be selected to match the average RDC of − 3.125 Hz. However, this approach could not be used to model D_{w1}, D_{w2}, D_{w3} or D_{w4} individually: these would have incorrect RDC values of − 3.125, − 1.752, −3.125 and − 1.752 Hz, respectively. The average of these RDCs is − 2.44 Hz, which is not equal to the correct average of − 3.125 Hz.

Alternatively, a D_a of 10.0 Hz could be selected to model the D_{w1} and D_{w3} values of −5.0 Hz, but the corresponding D_{w2} and D_{w4} values become − 2.97 Hz and the D_{ave} becomes

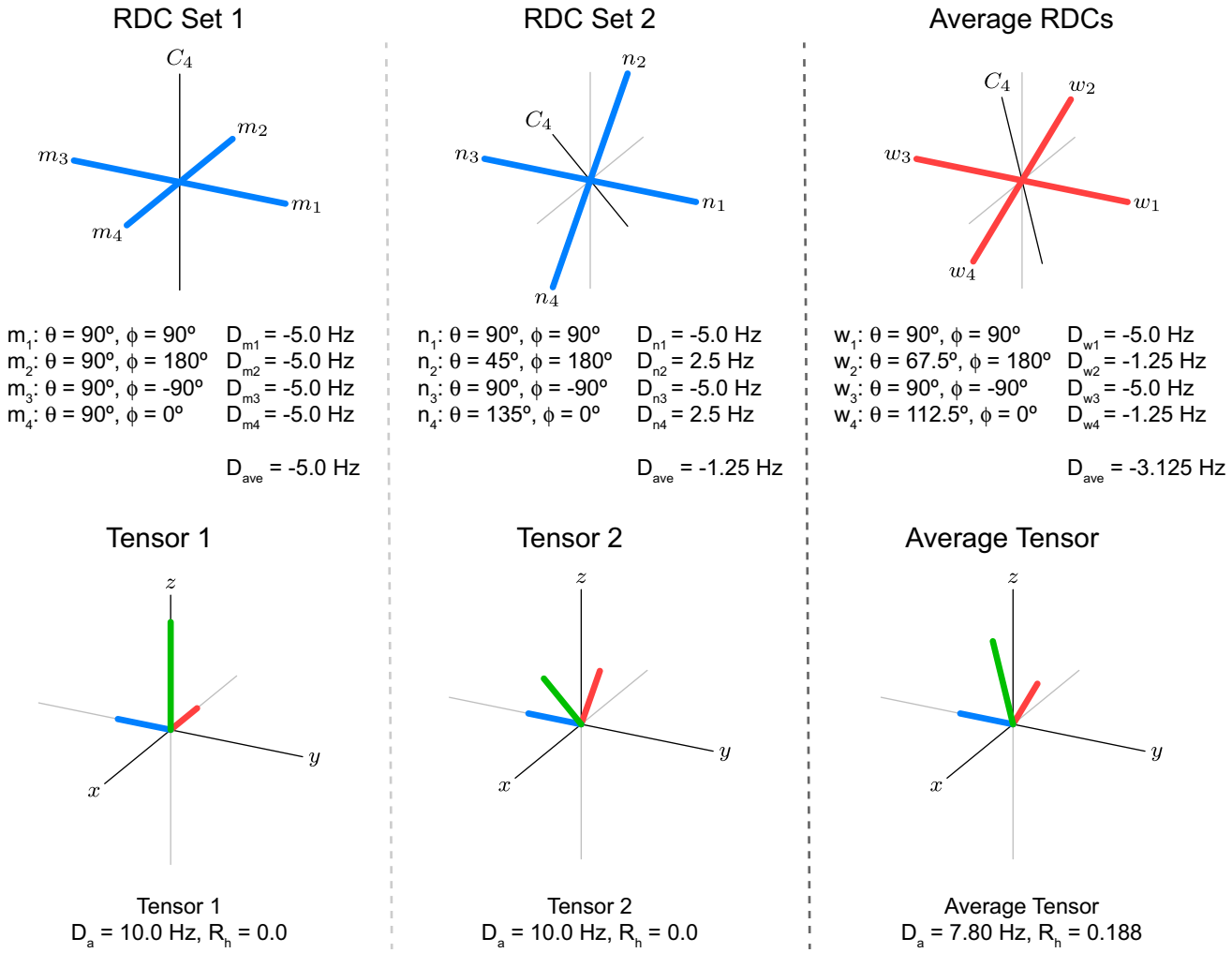

Fig. 1 Example of different alignments of a homotetramer with 1 bond per subunit. The orientations and RDCs for each bond in an alignment are presented under the molecule. For each alignment, the alignment tensor is shown on the bottom. The D_a and R_h of the alignment are indicated under their respective alignment tensors The average alignment represents the new alignment created by averaging RDC sets 1 and 2 with equal populations

– 3.902 Hz, which isn't correct either. Likewise, a D_a of 4.45 Hz could be used to model a – 1.25 Hz coupling for D_{w2} and D_{w4}, but then the corresponding D_{w1} and D_{w3} couplings are – 2.23 Hz and the D_{ave} is equal to – 1.74 Hz, which is incorrect as well.

Clearly, an axially symmetric alignment tensor is problematic, even for a single bond. The correct approach is to use an axially asymmetric alignment tensor, which can be calculated from the average of the alignment tensors for RDC sets 1 and 2.

The tensor, shown in red–blue–green in Fig. 1, represents the alignment tensor, as viewed from the fixed laboratory or alignment medium frame. The alignment tensor is defined by the molecular structure and how it interacts with the alignment medium.

RDC set 1 has an axially symmetric tensor (tensor 1, $\mathbf{T_1}$) with its principal axis oriented along the z-axis with a $D_a = 10.0$ Hz and $R_h = 0.0$.

$$\mathbf{T_1} = \begin{pmatrix} -5.0 & 0 & 0 \\ 0 & -5.0 & 0 \\ 0 & 0 & 10.0 \end{pmatrix} \text{Hz} \tag{6}$$

The tensor for RDC set 2 (tensor 2, $\mathbf{T_2}$) has a $D_a = 10.0$ Hz, and it is also axially symmetric ($R_h = 0$). Its principal axis is tilted by 45° away from the z-axis of the fixed coordinate system.

$$\mathbf{T_2} = \mathbf{R_y}(45°)\mathbf{T_1}\mathbf{R_y^{-1}}(45°)$$
$$\mathbf{T_2} = \begin{pmatrix} 2.5 & 0 & 7.5 \\ 0 & -5.0 & 0 \\ 7.5 & 0 & 2.5 \end{pmatrix} \text{Hz} \tag{7}$$

By averaging the 2 axially symmetric alignment tensors (tensor 1 and tensor 2) with equal populations, we produce a new axially asymmetric alignment average tensor ($\mathbf{T_{ave}}$) with a $D_a = 7.80$ Hz and $R_h = 0.188$. These parameters match the 2-site exchange parameters discussed below for a 22.5° half-angle of exchange (equation (30)).

$$\mathbf{T_{ave}} = \left(\mathbf{T_1} + \mathbf{T_2}\right)/2$$
$$\mathbf{T_{ave}} = \begin{pmatrix} -1.25 & 0 & 3.75 \\ 0 & -5.0 & 0 \\ 3.75 & 0 & 6.25 \end{pmatrix} \text{Hz} \tag{8}$$

The new average tensor, $\mathbf{T_{ave}}$, can be used to accurately model D_{w1}, D_{w2}, D_{w3} and D_{w4} as well as the average RDC, D_{ave}, from bond vectors w_1, w_2, w_3 and w_4.

$$\begin{aligned} D_{w1} =& (7.80\text{ Hz})\left\{ \tfrac{1}{2}\left(3\cos^2 90° - 1\right) \right. \\ & \left. + \tfrac{3}{4}(0.188)\sin^2 90° \cos 180° \right\} \\ =& -5.0\text{ Hz} \\ D_{w2} =& (7.80\text{ Hz})\left\{ \tfrac{1}{2}\left(3\cos^2 67.5° - 1\right) \right. \\ & \left. + \tfrac{3}{4}(0.188)\sin^2 67.5° \cos 360° \right\} \\ =& -1.25\text{ Hz} \\ D_{w3} =& (7.80\text{ Hz})\left\{ \tfrac{1}{2}\left(3\cos^2 90° - 1\right) \right. \\ & \left. + \tfrac{3}{4}(0.188)\sin^2 90° \cos(-180°) \right\} \\ =& -5.0\text{ Hz} \\ D_{w3} =& (7.80\text{ Hz})\left\{ \tfrac{1}{2}\left(3\cos^2 112.5° - 1\right) \right. \\ & \left. + \tfrac{3}{4}(0.188)\sin^2 112.5° \cos 0° \right\} \\ =& -1.25\text{ Hz} \end{aligned} \tag{9}$$

The molecular symmetry is also preserved in the averaged alignment. Rotation about the new C_4 axis produces the correct average RDC for the 4 bonds.

$$\begin{aligned} D_{ave} &= (-5.0\text{ Hz} + 1.25\text{ Hz} - 5.0\text{ Hz} + 1.25\text{ Hz})/4 \\ &= -3.125\text{ Hz} \end{aligned} \tag{10}$$

The average alignment tensor can also be calculated without knowledge or computation of the alignment tensors 1 and 2. RDCs for a total of 5 bonds can be calculated for RDC set 1, set 2 and an average set of RDCs in the tetramer (Table S1). A singular value decomposition (SVD) analysis of these RDCs shows that the $D_a = 7.80$ Hz and $R_h = 0.188$. The alignment tensor accurately models the RDC for each bond in each subunit as well as the average RDC for each bond, after accounting for the rotation about the C_4 axis.

In summary, we need an axially asymmetric tensor ($R_h \neq 0$) to accurately model the RDCs of a homotetramer with multiple alignment orientations.

Irreducible spherical tensors

The analysis of the alignment frame in partially aligned samples is typically conducted in a Cartesian basis (Losonczi et al. 1999; Bax et al. 2001). However, an irreducible spherical representation (Rose 1957; Steigel and Spiess 1978; Schmidt-Rohr and Spiess 1994) offers different advantages in the frame transformations of magnetic interactions for the analysis of partial alignment.

The first order RF Hamiltonian comprises a series of interactions, x, including dipolar and chemical shift interactions.

$$\mathcal{H}_{\text{RF}} = \sum_{x}^{\text{interactions}} \mathcal{H}_x \tag{11}$$

In the RF, the contribution from the Zeeman interaction is removed.

Each interaction has a spin tensor ($\mathbf{T}$) and a spatial tensor ($\mathbf{V}$) Steigel and Spiess (1978). In the irreducible spherical representation, the interaction Hamiltonian is written as follows.

$$\mathcal{H}_x = (V_{20}^{(\text{LAB})} T_{20} + V_{00} T_{00}) \tag{12}$$

Only the T_{20} and T_{00} components are secular with the Zeeman interaction and remain in the rotating frame Hamiltonian.

Tensors are grouped by their rotational properties and rank. V_{00} is the isotropic component, which is rotationally invariant (Steigel and Spiess 1978). There are 3 first rank, antisymmetric components, V_{1n}, with 'n' adopting values of − 1, 0 and 1. The first rank components do not contribute to the RF Hamiltonian. There are 5 second rank, symmetric components, V_{2m}, with 'm' adopting values of − 2, − 1, 0, 1 and 2. The second rank components depend on the orientation of the interaction with respect to the laboratory frame (LAB). The LAB frame is defined by the direction of the magnetic field, and it is conventionally selected as the z-axis.

Second rank and zeroth rank tensors in the irreducible spherical representation are converted to their Cartesian counterparts as follows (Schmidt-Rohr and Spiess 1994).

$$\begin{aligned} V_{20} &= \sqrt{\tfrac{3}{2}}(V_{zz} - V_{00}) \\ V_{2\pm2} &= \tfrac{1}{2}\{(V_{xx} - V_{yy}) \pm i(V_{xy} + V_{yx})\} \\ V_{00} &= \tfrac{1}{3}(V_{xx} + V_{yy} + V_{zz}) \end{aligned} \tag{13}$$

Magnetic interactions have an anisotropic symmetric contribution (T_{20}) and may have an isotropic contribution (T_{00}). Examples of magnetic interactions with an isotropic contribution are the chemical shift and J-coupling, whereas the dipolar coupling does not have an isotropic contribution—i.e. $T_{00}^{(\text{dipolar})} = 0$.

In the irreducible spherical representation, passive rotations are expressed using Wigner rotation matrices (**D**). A passive rotation involves the rotation of a coordinate system, whereas an active rotation rotates an object in a fixed coordinate system (Schmidt-Rohr and Spiess 1994). A single coordinate transformation from a coordinate system 'A' to 'B' is conducted using the Euler angles α, β and γ.

$$V_{2m}^{(\text{B})} = \sum_{m=-2}^{m=2} V_{20}^{(\text{A})} D_{0m}^{(2)}(0, \beta, \gamma) \tag{14}$$

The V_{20} component represents the principal component of the second rank tensor, and $\mathbf{D}^{(2)}$ is the Wigner matrix of second rank. Since we are exclusively using Wigner rotation matrices of second rank, and these are summed in integer increments from $m = -2$ to $m = 2$, we will use the following simplified notation to represent a rotation from frame 'A' to frame 'B'.

$$V_{2m}^{(\text{B})} = \sum_{m} V_{20}^{(\text{A})} D_{0m}^{AB}(0, \beta, \gamma) \tag{15}$$

In this case, we are rotating an axially symmetric tensor—i.e. $V_{2\pm2} = 0$ and $V_{xx} = V_{yy}$.

Dipolar interactions

The dipolar coupling is measured between spins 'p' and 'q'. In the Cartesian representation, the angular frequency (ω_{pq}) and frequency ($V_{zz}^{(\text{PAS})}$) of the dipolar coupling are evaluated as follows.

$$\begin{aligned} \omega_{pq}^{(PAS)} &= -\frac{\mu_0 \hbar \gamma_p \gamma_q}{4\pi r_{pq}^3} \\ V_{zz}^{(\text{PAS})} &= -\frac{\mu_0 \hbar \gamma_p \gamma_q}{8\pi^2 r_{pq}^3} \end{aligned} \tag{16}$$

The tensor is expressed in its Principal Axis System (PAS) in which the tensor is diagonal. $V_{zz}^{(\text{PAS})}$ is the principal component of the tensor, and it is colinear with the internuclear vector. μ_0 is the vacuum permittivity, $\hbar$ is the Planck constant, γ_p and γ_q are the gyromagnetic ratios for spins 'p' and 'q', respectively, and r_{pq} is the internuclear distance between spins 'p' and 'q.'

For an ^{1}H–^{15}N bond of 1.02 Å, $V_{zz}^{(\text{PAS})}$ has a value of +11.5 kHz, and for an ^{1}H–^{13}C bond of 1.10 Å, $V_{zz}^{(\text{PAS})}$ has a value of −22.7 kHz. Respecting the sign of $V_{zz}^{(\text{PAS})}$ is important when fitting RACSs (Lorieau 2017).

In the analysis of the spatial dependence of magnetic interactions in a molecule, the spatial part of a dipolar coupling interaction must at least be transformed from its PAS to the frame of the molecule (MOL), then to the LAB frame.

$$V_{20}^{(\text{LAB})} = \sum_{m} V_{20}^{(\text{PAS})} D_{0m}^{\text{PM}}(0, \theta, \phi) D_{m0}^{\text{ML}}(\alpha, \beta, 0) \tag{17}$$

The first transformation is conducted by the D_{0m}^{PM} components, and the second transformation is conducted by the D_{m0}^{ML} components. We only keep the $V_{20}^{(\text{LAB})}$ component since it is the only secular component with the Zeeman Hamiltonian (Steigel and Spiess 1978).

Altogether, there are 5 terms. We evaluate equation (17) to find its orientational dependency.

$$\begin{aligned} V_{20}^{(\text{LAB})} =& V_{20}^{(\text{PAS})} \left\{ \tfrac{1}{4}\left(3\cos^2\theta - 1\right)\left(3\cos^2\beta - 1\right) \right. \\ & \left. + \tfrac{3}{4}\sin^2\theta \cos 2\phi \sin^2\beta \cos 2\alpha \right\} \end{aligned} \tag{18}$$

The $m = \pm 1$ terms have opposite sign and cancel.

In a rigid molecule, the angles θ and ϕ are fixed by the structure of the molecule. For a crystalline sample in the solid state, the dipolar interaction contributes directly to the spectrum with a value that depends on the orientation of the molecule with respect to the laboratory frame, α and β. Additionally, the number of interactions oriented at an angle (α, β) are integrated over the population $p(\alpha, \beta)$. For molecules distributed randomly and uniformly on a sphere, the probability, $p(\alpha, \beta)$, is equal to '$\sin\beta$' because there are more equatorial orientations in a sphere than polar orientations.

In the solution state, molecules tumble (rotate) isotropically on a rapid timescale (ps-ns). Consequently, only an average over the orientations α and β is measured.

$$\begin{aligned} \left\langle V_{20}^{(\text{LAB})} \right\rangle &= \left\langle \sum_{m} V_{20}^{(\text{PAS})} p(\alpha, \beta) D_{0m}^{\text{PM}}(0, \theta, \phi) D_{m0}^{\text{ML}}(\alpha, \beta, 0) \right\rangle \\ &= V_{20}^{(\text{PAS})} \left\{ \int_{\beta=0}^{\pi} \mathrm{d}\beta \cdot \sin\beta \tfrac{1}{4}\left(3\cos^2\theta - 1\right)\left(3\cos^2\beta - 1\right)/\pi \right. \\ &\quad \left. + \iint_{\alpha=0,\beta=0}^{2\pi,\pi} \mathrm{d}\alpha \mathrm{d}\beta \cdot \sin\beta \tfrac{3}{4}\sin^2\theta \cos 2\phi \sin^2\beta \cos 2\alpha / 2\pi^2 \right\} \\ &= 0 \end{aligned} \tag{19}$$

The angle brackets represent a time and ensemble average. The time average is zero for the dipolar interaction experiencing isotropic rotational diffusion. It is for this reason that dipolar interactions are not directly measured in a solution NMR spectrum.

Partial alignment reintroduces the anisotropic component of magnetic interactions by biasing the molecular orientations from an isotropic distribution to a slightly anisotropic distribution.

Partial alignment

In a partially aligned sample, the $p(\alpha, \beta)$ probabilities depart from a 'sin β' distribution. The functional dependence of $p(\alpha, \beta)$ may be quite complicated, as it depends on the nature of the alignment, the structure of the molecule and, potentially, the electrostatic distribution and shape of the molecule (Zweckstetter and Bax 2000; Zweckstetter et al. 2004).

At this stage, we will make a simplifying observation on the nature of $p(\alpha, \beta)$. In a weakly aligned sample, the orientational distribution of molecules is largely the same as an isotropic sample. Nevertheless, some orientations may be more likely than others. It is then convenient to convert the integral in equation (19) to a discrete sum for a small subset of partially aligned orientations. Most orientations and their probabilities are isotropic, and the corresponding dipolar couplings are mutually canceled, while some orientations 'i' are favored in a partially aligned sample. This approach is analogous to the steric obstruction and electrostatic modeling of the alignment tensor (Zweckstetter and Bax 2000; Zweckstetter et al. 2004).

We will focus on the discrete orientations, which are not canceled.

$$\left\langle V_{20}^{(\mathrm{LAB})} \right\rangle = \sum_{i}^{\mathrm{N}} p(\alpha_i, \beta_i) \cdot V_{20}^{(\mathrm{PAS})} \left\{ \tfrac{1}{4}\left(3\cos^2\theta - 1\right)\left(3\cos^2\beta_i - 1\right) + \tfrac{3}{4}\sin^2\theta\cos 2\phi \sin^2\beta_i \cos 2\alpha_i \right\} \tag{20}$$

The sum is conducted over 'N' partially aligned orientations 'i'. In the simplest case, the partially aligned molecule is biased to a single orientation ($N = 1$). As we will see below, biomolecules often align with multiple orientations ($N > 1$).

Uniaxial alignment

Partial alignment is commonly introduced with a liquid crystal or a distorted gel (Tjandra and Bax 1997; Tycko et al. 2000; Hansen et al. 1998). Alignment media in NMR typically introduce uniaxial alignment. A liquid crystal, for example, aligns in a magnetic field based on its diamagnetic anisotropy susceptibility (Dong 1997). For uniaxial alignment, ordering occurs along one axis while orthogonal orientations are disordered. Consequently, we must include a frame transformation for the alignment medium itself (D_{n0}^{AL}).

$$\left\langle V_{20}^{(\mathrm{LAB})} \right\rangle = \sum_{i}^{N} \sum_{m,n} \left\{ p(\alpha_i, \beta_i, \gamma_i) V_{20}^{(\mathrm{PAS})} \cdot D_{0m}^{\mathrm{PM}}(0, \theta, \phi) D_{mn}^{\mathrm{MA}}(\alpha_i, \beta_i, \gamma_i) D_{n0}^{\mathrm{AL}}(\alpha_{\mathrm{AL}}(t), \beta_{\mathrm{AL}}, 0) \right\} \tag{21}$$

The dipolar tensor is transformed from the PAS to the molecular frame (D_{0m}^{PM}) by the orientation of internuclear vectors or chemical shift tensors in the molecule. Thereafter, the tensor is transformed from the molecular to the alignment frame (D_{mn}^{MA}) through the different orientations between the molecule and the alignment medium. Finally, the dipolar tensor is transformed from the alignment frame to the laboratory frame (D_{n0}^{AL}).

For uniaxial alignment, the alignment medium is ordered in β_{AL}, with respect to the axis of the magnetic field, and diffuses isotropically about the $\alpha_{\mathrm{AL}}(t)$ angle. As a result, only the time average of the alignment frame is measured.

$$\begin{aligned} \left\langle V_{20}^{(\mathrm{LAB})} \right\rangle &= \sum_{i}^{N} \sum_{m,n} \left\{ p(\alpha_i, \beta_i, \gamma_i) V_{20}^{(\mathrm{PAS})} \right. \\ &\quad \cdot D_{0m}^{\mathrm{PM}}(0, \theta, \phi) D_{mn}^{\mathrm{MA}}(\alpha_i, \beta_i, \gamma_i) \\ &\quad \left. \left\langle D_{n0}^{\mathrm{AL}}(\alpha_{\mathrm{AL}}(t), \beta_{\mathrm{AL}}, 0) \right\rangle \right\} \\ &= \sum_{i}^{N} \sum_{m} \left\{ p(\alpha_i, \beta_i) V_{20}^{(\mathrm{PAS})} \right. \\ &\quad \left. D_{0m}^{\mathrm{PM}}(0, \theta, \phi) D_{m0}^{\mathrm{MA}}(\alpha_i, \beta_i, 0) \left\langle d_{00}^{\mathrm{AL}}(\beta_{\mathrm{AL}}) \right\rangle \right\} \end{aligned} \tag{22}$$

The uniaxial averaging of the alignment medium eliminates the dependence on the γ_i Euler angle between the molecule and the alignment frame.

The final expression for uniaxial partial alignment includes a simple scaling constant for the alignment medium, $\left\langle d_{00}^{\mathrm{AL}}(\beta_{\mathrm{AL}}) \right\rangle$. This term represents the degree of alignment for the alignment medium itself, and it can be represented by an order parameter (S_{AL}). The order parameter value ranges from 1 to −0.5, excluding values near zero. Crystals that do not order have S_{AL} parameters near zero and do not produce RDCs or RACS.

The RDC equation

In the structural refinement of molecules using partially aligned data, like RDCs or RACSs, we are interested in the

θ and ϕ orientations, which relate the orientation of a particular dipole interaction to its molecular frame.

First, we re-factor equation (22) to isolate the motional averaging between the molecule and the alignment frame. The exchange between these orientations is rapid on the timescale of the free induction decay (FID) evolution, and only an average is measured.

$$\left\langle V_{20}^{(\mathrm{LAB})} \right\rangle = \sum_m V_{20}^{(\mathrm{PAS})} D_{0m}^{\mathrm{PM}}(0,\theta,\phi) \left\langle \sum_i^N p(\alpha_i,\beta_i) D_{m0}^{\mathrm{MA}}(\alpha_i,\beta_i,0) \right\rangle S_{AL} \tag{23}$$

For a molecular structure with an arbitrary initial orientation, the alignment is defined by 5 or fewer components 'm'. Together, these form the 5 components of the Saupe matrixSaupe (1968). The Saupe matrix in the irreducible spherical representation is derived in the Supplemental Information.

Alternatively, we may select the α and β orientations for a molecular frame in which the $m = \pm 1$ terms are zero. This is the principal axis system of the alignment frame.

$$\begin{aligned}\left\langle V_{20}^{(\mathrm{LAB})} \right\rangle =& V_{20}^{(\mathrm{PAS})} \tfrac{1}{2}\left(3\cos^2\theta - 1\right) S_{\mathrm{AL}} \left\langle \sum_i^{\mathrm{N}} p(\alpha_i,\beta_i) \cdot \tfrac{1}{2}\left(3\cos^2\beta_i - 1\right) \right\rangle \\ &+ V_{20}^{(\mathrm{PAS})} \sin^2\theta\cos 2\phi S_{\mathrm{AL}} \left\langle \sum_i^{\mathrm{N}} p(\alpha_i,\beta_i) \cdot \tfrac{3}{4}\sin^2\beta_i \cos 2\alpha_i \right\rangle\end{aligned} \tag{24}$$

The terms with the molecular orientations, α_i and β_i, and probabilities, $p(\alpha_i,\beta_i)$, are averaged together in the alignment of the molecule. These represent the different orientations of partial alignment of a molecule. Figure 2 shows an example of a monomeric molecule of arbitrary shape with 2 interaction orientations with populations p_1 and p_2.

The partial alignment may arise from electrostatic interactions, in which case a negatively charged alignment medium (the line in red) may orient patches of positive charge (drawn as blue patches on the gray molecule). This example molecule orients with respect to the alignment medium with 2 different sets of angles and 2 different populations. One orientation (p_2) is more favored in this example, but both contribute to the average alignment tensor or frame. Altogether, the 2 orientations produce the average tensor components in Eq. (24). However, the α_i and β_i angles are defined in relation to the final diagonal alignment frame.

In the RDC equation, the principal component of the interaction, $V_{20}^{(\mathrm{PAS})}$, is constant for a molecule that is internally rigid.

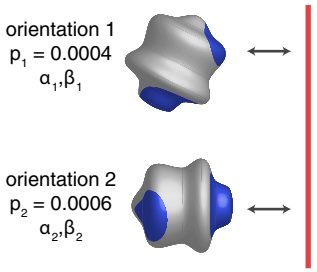

Fig. 2 Example alignment of a monomeric molecule (drawn in gray) interacting with an alignment medium (red line). This molecule has 2 regions of interaction (drawn in blue), producing an alignment with 2 sets of orientations with respect to the alignment medium and frame. The first interaction orientation has the α_1 and β_1 Euler angles and population $p_1 = 0.0004$, and the second interaction orientation has the α_2 and β_2 Euler angles and population $p_2 = 0.0006$. In a more realistic example, each of these interaction orientations would represent a manifold of sub-orientations with small local changes in orientation with respect to the alignment medium

When grouped together, Eq. (24) has terms proportional to $(3\cos^2\theta - 1)$ and terms proportional to $(\sin^2\theta\cos 2\phi)$.

There are 2 conventions to describe the orientation dependence of dipolar couplings in the partial alignment and solid-state NMR literature. The first defines the averaged dipolar coupling in terms of an asymmetry parameter, η Torchia (2015). We will use the other convention originally used in the RDC literature, which orders the alignment tensor components as $|A_{zz}| \geq |A_{yy}| \geq |A_{xx}|$ and describes asymmetry in the alignment tensor with a rhombicity, R_h (Bax 2003; Clore and Garrett 1999). The RDC equation is expressed as follows.

$$D(\theta_j,\phi_j) = D_a\left\{\left(3\cos^2\theta_j - 1\right) + \tfrac{3}{2}R_h\sin^2\theta_j\cos 2\phi_j\right\} \tag{25}$$

By convention, this equation is different from Eq. (1) because a factor $\frac{1}{2}$ is included in the D_a.

In a rigid molecule, the molecular alignment parameters (D_a and R_h) are common to all magnetic interactions of the same type, and equation (25) can be used to fit multiple RDCs or axially symmetric RACSs values 'j'. The D_a and R_h are defined in relation to the alignment tensor components.

$$\begin{aligned} D_a &= \sqrt{\tfrac{3}{8}} D_{zz}^{(\mathrm{PAS})} A_a \\ R_h &= \frac{2}{3}\frac{A_r}{A_a} \end{aligned} \tag{26}$$

These components can be determined in relation to Eq. (24).

$$\begin{aligned} A_a = A_{zz} &= S_{AL}\left\langle \sum_i^{\mathrm{N}} p(\alpha_i,\beta_i) \cdot \tfrac{1}{2}\left(3\cos^2\beta_i - 1\right) \right\rangle \\ A_r = A_{xx} - A_{yy} &= S_{AL}\left\langle \sum_i^{\mathrm{N}} p(\alpha_i,\beta_i) \tfrac{3}{2}\sin^2\beta_i\cos 2\alpha_i \right\rangle \end{aligned} \tag{27}$$

The rhombicity (R_h) varies within the range of [0, 2 / 3]. An axially symmetric alignment tensor has an $R_h = 0$ whereas an axially asymmetric alignment tensor has a non-zero rhombicity, $R_h \neq 0$.

In cases where there is motion within the molecule, particularly for molecules with flexible domains or loops, the alignment parameters D_a and R_h may be different for different parts of the molecule.

The rhombicity of the alignment tensor has a special significance in the context of the partial alignment for molecules with symmetry. Importantly, a chiral monomeric molecule that has only 1 interaction orientation will only produce axially symmetric alignment—i.e. $R_h = 0$. In the context of Fig. 2, this would represent a molecule with only 1 interaction patch, instead of 2, and only 1 orientation with respect to the alignment frame.

If an internally rigid molecule interacts with the alignment medium with only one orientation, the alignment and molecular frames are the same such that $\alpha = 0$, $\beta = 0$, and the alignment tensor is axially symmetric—i.e. $R_h = 0$.

$$D(\theta_j) = D_a\left(3\cos^2\theta_j - 1\right) \tag{28}$$

A non-zero R_h indicates that a monomeric molecule interacts with the alignment medium with more than one distinct orientation. However, since the interaction with the alignment medium is typically non-specific, particularly for a large biomolecule, a single interaction with the alignment would be unusual.

The impact of molecular symmetry

A molecule may have symmetry point groups and bear symmetry in the alignment. In some cases, this symmetry may produce simplified relationships with the alignment frame. Biomolecules, for instance, may form homo-oligomers with C_n symmetries.

In the original report by Saupe (1968), simple relationships are identified in the alignment matrix of symmetric molecules. Small molecules with a 3-fold axis of symmetry are found to produce axially symmetric alignment tensors ($R_h = 0$). In the context of the above discussion, this is correct for the alignment of simple molecules, like benzene and 1,3,5-trichlorobenzene, which interact with the alignment medium with only one orientation for each symmetric orientation. For larger molecules, like biomolecules that may interact and orient with the alignment medium in different ways, these simplified relationships may break down. For example, a protein may have arginine and lysine residues on different regions of the surface of the molecule. These residues produce multiple positively-charged surfaces, which interact and align with different orientations in a negatively-charged alignment medium, such as Pf1 phage of d(GpG) (Hansen et al. 1998; Lorieau et al. 2008).

The impact of symmetry on the alignment frame can be evaluated directly from the averaging orientations in Eqs. (26) and (27). The molecule may adopt a set of *symmetry orientations* based on the rotation about an axis of symmetry, and the molecule may adopt a series of *interaction orientations* for each symmetry orientation. Generally, interaction orientations that change the orientation of the symmetry axis may produce axially asymmetric alignment tensors for homo-oligomers with 2 or more subunits.

Monomers and non-symmetric molecules

The simplest system is a monomeric or non-symmetric molecule with only one symmetry orientation and one interaction orientation. In this case, the alignment and molecular frames are the same such that $\alpha = 0°$ and $\beta = 0°$. The alignment tensor is axially symmetric, according to Eqs. (26) and (27).

$$\begin{aligned} D_a &= \tfrac{1}{2}D_{zz}^{(\mathrm{PAS})}p \\ R_h &= 0 \end{aligned} \tag{29}$$

The population 'p' represents the single orientation that is biased in partially aligning the molecule, and it is typically on the order of 10^{-3}. The R_h for a single orientation is zero (Fig. 3a).

A single interaction is highly specific. Common alignment media orient based on molecular shape and steric occlusion, the electrostatic surface potential of the molecule or both factors together (Zweckstetter et al. 2004; Zweckstetter and Bax 2000). These are non-specific interactions, and more commonly, molecules adopt many interaction orientations in an alignment medium, like the 2 interaction orientations shown for a monomer in Fig. 2.

The more common case involves the non-specific alignment of a molecule with many interaction orientations. This type of alignment (Fig. 3b) typically produces non-zero R_h values and axially asymmetric alignment tensors—though multiple interaction orientations may fortuitously produce a zero R_h as well. RDC datasets for monomers commonly have non-zero R_h values.

For example, RDC datasets in many different alignment media are available for ubiquitin, a monomer. The alignment rhombicity, R_h, is 0.08 and 0.60 for squalamine and bicelle alignment media (Cornilescu et al. 1998; Cornilescu and Bax 2000; Maltsev et al. 2014), respectively, indicating that ubiquitin monomers have multiple interaction orientations with these alignment media.

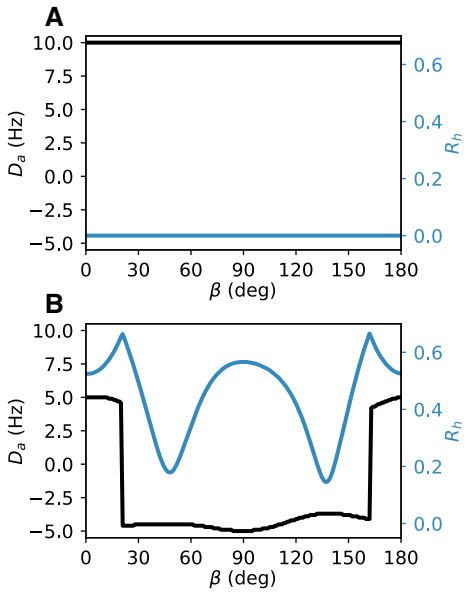

Fig. 3 Simulated ^{1}H–^{15}N RDC alignment tensor parameters, D_a and R_h, for ubiquitin, a monomer. Two rotations are conducted in generating the RDCs: first an interaction rotation, then a single symmetry rotation about an azimuthal angle β. **a** A single interaction orientation with Euler angles $(30°, 30°, 30°)$ and different azimuthal angles β. **b** Multiple interaction orientations with Euler angles of $(0°, 0°, 0°)$, $(30°, 30°, 30°)$, $(60°, 60°, 60°)$ and $(90°, 90°, 90°)$ with equal populations. The RDCs were simulated with a D_a of 10 Hz

Homodimers, C_2 and D_2 symmetries and 2-site averaging

Molecules with C_2 symmetry rotate between symmetry orientations $\alpha = 0°$ and $\alpha = 180°$ about a polar angle β. In the solid-state NMR literature, this type of tensor averaging is known as a 2-site hop or 2-site exchange (Sarkar et al. 1986). The populations of the two orientations are equal for a homodimer ($p_1 = p_2 = 0.5$).

The reorientation angle β depends on the nature of the alignment, and either the shape, electrostatic distribution or other factors of the dimer. Figure 4 shows two examples of homodimers with reorientation angles of $\beta = 0°$ and $\beta = 58°$.

The simplest case is a dimer molecule with only 1 interaction orientation. To evaluate the tensor components for 2-site averaging, the components of the averaged alignment matrix from Eq. (27) are evaluated as follows.

$$\begin{aligned} A_a &= 2p \cdot S_{\mathrm{AL}} \tfrac{1}{2}\left(3\cos^2\beta - 1\right) \\ A_r &= 2p \cdot S_{\mathrm{AL}} \tfrac{3}{2}\sin^2\beta \end{aligned} \tag{30}$$

The new alignment matrix cannot be used directly to calculate the D_a and R_h, since the order of the A_{xx}, A_{yy} and A_{zz} components change with different values of βSarkar et al. (1986). Instead, the 3 components should be evaluated separately.

$$\begin{aligned} A_{zz} &= 2p \cdot S_{\mathrm{AL}}\left(\tfrac{3}{2}\cos^2\beta - \tfrac{1}{2}\right) \\ A_{xx} &= 2p \cdot S_{\mathrm{AL}}\left(\tfrac{3}{2}\sin^2\beta - \tfrac{1}{2}\right) \\ A_{yy} &= 2p \cdot S_{\mathrm{AL}}\left(-\tfrac{1}{2}\right) \end{aligned} \tag{31}$$

The A_{yy} component remains unchanged because the β rotation occurs about this axis.

Figure 5 shows how the alignment D_a and R_h vary with the jump angle β. For a simple 2-site exchange, there are

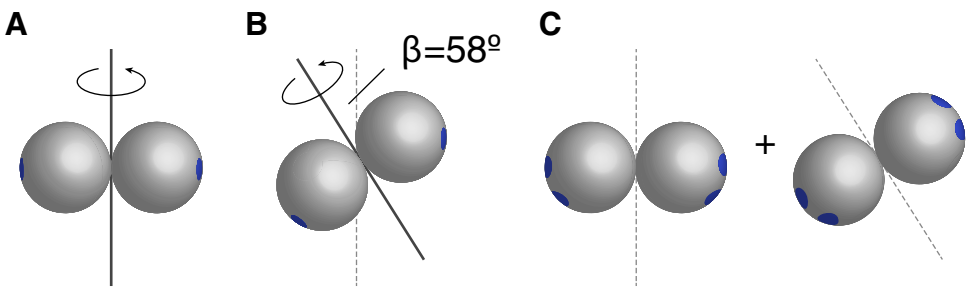

Fig. 4 Diagram for exchange examples with homodimers. **a** A homodimer with 1 interaction orientation and 2 symmetry orientations. The homodimer is represented by 2 spheres that rotate between 2 orientations about the symmetry axis, drawn as a solid line. Each subunit of the homodimer has one interaction patch (labeled in blue). The patch interacts with an alignment medium oriented vertically. The homodimer orientations exchange about an angle $\beta = 0°$. **b** A homodimer with 1 interaction and 2 symmetry orientations, with the symmetry orientations exchanging about an angle $\beta = 58°$. **c** A homodimer with 2 interaction orientations, each with 2 symmetry orientations. The average alignment frame is defined by the average of 4 orientations

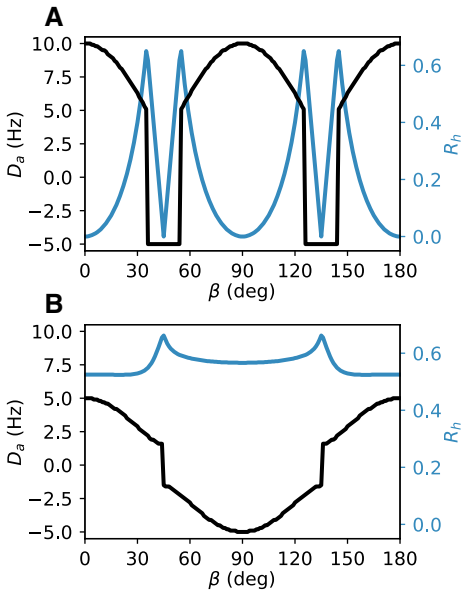

Fig. 5 Simulated ^{1}H–^{15}N RDC alignment tensor parameters, D_a and R_h, for ubiquitin subject to 2-site exchange. Two rotations are conducted in generating the RDCs: first an interaction rotation, then a 2-site symmetry rotation about an azimuthal angle β. **a** A simple 2-site exchange with 1 interaction orientation with Euler angles $(0°, 0°, 0°)$ between the molecular and alignment frames. The D_a and R_h are plotted for different azimuthal angles of rotation, β, about the C_2 axis and each symmetric orientation has an equal population. **b** The 2-site exchange for ubiquitin molecules adopting interaction orientations with Euler angles $(0°, 0°, 0°)$, $(30°, 30°, 30°)$, $(60°, 60°, 60°)$ and $(90°, 90°, 90°)$. Each orientation has an equal population. The RDCs were simulated with a D_a of 10 Hz

discontinuities at *ca.* 35.26° ($\arccos\sqrt{2/3}$) and *ca.* 54.74° ($\arccos\sqrt{1/3}$) because the A_{yy} component becomes the dominant and principal component in this range.

At β values of 0° and 90°, the R_h is equal to 0. For 25% of the β orientations, the R_h is small (< 0.033) and may appear to be axially symmetric. Molecules with D_2 symmetry are represented by a β angle of 180°.

In Fig. 5b, the alignment tensor parameters from simulated RDCs in ubiquitin are shown for molecules visiting four interaction orientations. The interaction orientations have equal probabilities and each has 2 symmetry orientations. Altogether, there are 16 orientations each with a population of 1 / 16. If the molecule visits multiple interaction orientations for each site, the D_a and R_h are different from the 2-site, 1 interaction orientation model (Fig. 5a). Equation (27) cannot be used directly since we have two separate sets of rotations. These rotations also cannot be combined by adding the α and β angles since rotations about orthogonal axes are non-commutable. See the Methods section for details.

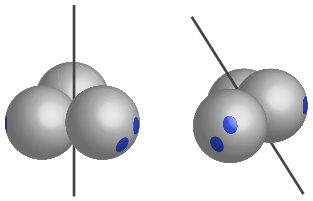

Fig. 6 Diagram for exchange examples with homotrimers. The homotrimer is represented by 3 spheres with a symmetry axis, drawn as a solid grey line. The homotrimer has subunits with 2 interaction patches (labeled in blue) such that the symmetry axis may form an angle of $\beta = 0°$ or $\beta = 58°$ with respect to the alignment medium. The average alignment frame is defined by the average of 6 orientations constructed from 3 symmetry orientations and 2 interaction orientations

With this simulation, and the simple 2-site exchange in Fig. 5a, there appears to be no simple way to detect a homodimer from the alignment tensor D_a or R_h.

Homo-oligomers with C_n and D_n symmetries

Molecules with C_n symmetries rotate between 'n' molecular orientations α_i about a polar angle β. The populations of each state are equal for homo-oligomers. Example molecules are homotrimeric, homotetrameric and homopentameric proteins.

Like homodimers and molecules with C_2 symmetries, the angle β depends on the nature of the alignment and the axis of symmetry. In this case, the A_{zz} component remains the principal component, and equations (26) and (27) can be used directly for molecules with 1 interaction orientation.

$$\begin{aligned} D_a &= np \cdot S_{\mathrm{AL}} \tfrac{1}{2}\left(3\cos^2\beta - 1\right) \\ R_h &= 0 \end{aligned} \tag{32}$$

In this case, the alignment tensor is axially symmetric ($R_h = 0$). However, conclusions based on the value of R_h can be perilous, given that multiple interaction orientations may be present (Fig. 6).

In the monomer case, we saw that multiple interaction orientations are needed to produce an axially asymmetric alignment tensor ($R_h \neq 0$). Given the frequency of axially asymmetric alignment tensors for monomers, monomers frequently interact with the alignment medium with multiple interaction orientations. Likewise, a homo-oligomer, like a trimer, may have subunits that have multiple interaction orientations with the alignment medium. Multiple interaction orientations in a homo-oligomer would preserve the symmetry of the homo-oligomer, yet it would potentially produce a non-zero R_h in the alignment tensor.

In the simulated alignment in Fig. 7a, ubiquitin molecules align with symmetry orientations for a 3-site exchange.

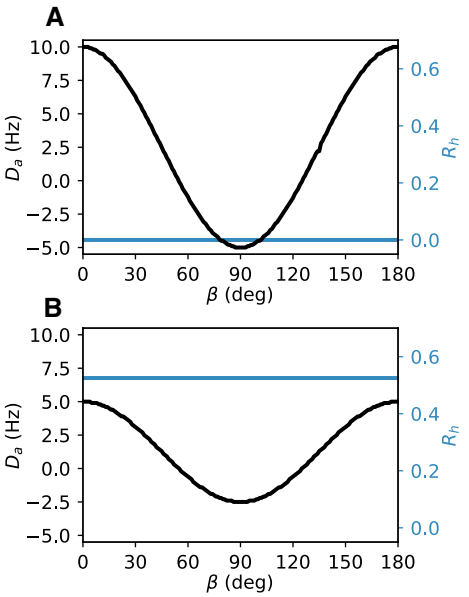

Fig. 7 Simulated ^{1}H–^{15}N RDC alignment tensor parameters, D_a and R_h, for ubiquitin subject to 3-site exchange. Two rotations are conducted in generating the RDCs: first an interaction rotation, then a 3-site symmetry rotation about an azimuthal angle β. **a** A simple 3-site exchange with 1 interaction orientation with Euler angles $(30°, 30°, 30°)$. The D_a and R_h are plotted for different azimuthal angles of rotation, β, about the C_3 axis and each symmetric orientation has an equal population. **b** The 3-site exchange for ubiquitin molecules adopting 4 interaction orientations with Euler angles $(0°, 0°, 0°)$, $(30°, 30°, 30°)$, $(60°, 60°, 60°)$ and $(90°, 90°, 90°)$ with each orientation experiencing a 3-site exchange of equal population. The RDCs were simulated with a D_a of 10 Hz. The source code for this simulation is included in the Supplementary Information

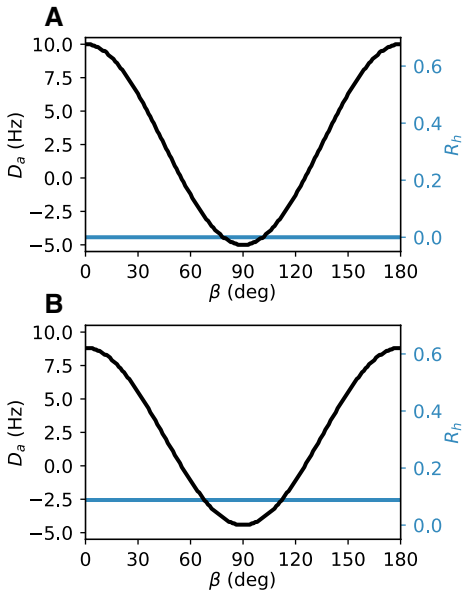

Fig. 8 Simulated ^{1}H–^{15}N RDC alignment tensor parameters, D_a and R_h, for ubiquitin subject to 3-site exchange with a narrow set of interaction orientations. Two rotations are conducted in generating the RDCs: first an interaction rotation, then a 3-site symmetry rotation about an azimuthal angle β. **a** A 3-site exchange with 3 interaction orientations with Euler angles $(40°, 0°, 0°)$, $(60°, 0°, 0°)$ and $(80°, 0°, 0°)$. The D_a and R_h are plotted for different azimuthal angles of rotation, β, about the C_3 axis and each symmetric orientation has an equal population. **b** A 3-site exchange with 3 interaction orientations with Euler angles $(0°, 40°, 0°)$, $(0°, 60°, 0°)$ and $(0°, 80°, 0°)$. The RDCs were simulated with a D_a of 10 Hz

There is only 1 interaction orientation, and R_h is consistently zero, as predicted by theory (Saupe 1968). Molecules with D_n symmetries are represented by a β value of 180°.

Figure 7b shows how 4 interaction orientations reduce the D_a and produce an axially asymmetric alignment tensor ($R_h \neq 0$). If an axially symmetric alignment tensor is expected for this system, and an axially asymmetric alignment tensor is measured, the experimentalist may incorrectly conclude that the protein forms a monomer instead of a trimer.

This situation is analogous to the motional averaging of methyl deuterons in crystalline L-[ϵ-$^{2}H_3$]-methionine (Keniry et al. 1983; Torchia 1984). Below the threshold temperature of − 10 °C, the ^{2}H quadrupolar tensor is axially symmetric and scaled by *ca.* 1 / 3 due to rotation of the methyl group. Above the threshold temperature, side-chain reorientations introduce additional motion to the methyl group and reorient the C_3 symmetry axis. As a result, an axially asymmetric ($R_h \neq 0$) average quadrupolar tensor and powder line-shape is measured. The axially symmetric alignment tensor of the $^{2}H_3C$ group is averaged between multiple orientations to produce an axially asymmetry tensor.

The interaction orientations of homo-oligomers may nevertheless have a more narrow distribution of interaction orientations than a monomeric molecule. This is because parts of the molecule are occluded by neighboring subunits. Figure 8 shows how the D_a and R_h vary for different 3-site hop models that have a narrow distribution (±20°) in the interaction orientations for the α (Fig. 8a) or β Euler angles (Fig. 8b). Even with narrow distributions in interaction orientations, it can be difficult to ascertain the oligomeric state of molecules based on the values of D_a and R_h.

Figure 8 shows how a change in the orientation of the symmetry axis is needed to produce a non-zero rhombicity. When only the α angle changes in the interaction orientation (Fig. 8a), the R_h remains zero. In this case, the 3-site hop is equivalent to a 9-site hop for the 3 interaction orientations and 3 symmetry orientations. It is only when the angle of the symmetry axis changes in Fig. 8b that the R_h becomes non-zero ($R_h = 0.088$).

Discussion

Homo-oligomers in the literature

In the current literature, there is a limited set of examples for RDCs and alignment tensor parameters of homo-oligomers.

The membrane proximal external region (MPER) of the HIV-1 gp41 protein is an example of a homotrimer with RDCs (Reardon et al. 2014). The MPER construct used in the study included an N-terminal trimerization domain, foldon (Saupe 1968), and its trimeric state was confirmed by analytic ultracentrifugation (AUC). The alignment tensor from HN RDCs had an $R_h = 0.052$, which the authors argue is nearly zero and consistent with a C_3 axis of symmetry. It appears that this is a case in which there is 1 interaction orientation or a set of interaction orientations with a very narrow distribution. Nevertheless, this partial alignment dataset only includes HN RDCs. For transmembrane helices, the HN bonds are oriented in nearly the same direction. Accurately defining the alignment tensor parameters can be difficult from a partial alignment dataset that does not samples all orientations in a sphere.

In another set of examples, the M2 homotetramer and phospholamban (PLN) homopentamer have axially asymmetric alignment tensors from RDC data. In stretched acrylamide gel (SAG), the M2 tetramer has an $R_h = 0.20$ and the PLN pentamer has an $R_h = 0.33$ (Schnell and Chou 2008; Oxenoid and Chou 2005). In the case of 1 interaction orientation, a homotetramer with a C_4 axis of symmetry and a homopentamer with a C_5 axis of symmetry would both produce axially symmetric tensors–i.e. $R_h = 0$. To justify the non-zero R_h values measured, the authors argue that molecular dynamics are impacting their tensor values. Indeed, dynamics slower than the exchange timescale between the protein and the alignment would break the symmetry of the molecule. In the absence of such motions, these systems may also present multiple interaction orientations to produce an axially asymmetric alignment tensor.

These two structures are also the subject of debate. The M2 tetrameric structure was collected in dihexanoylphosphatidylcholine (DHPC) micelles, which may have impacted the orientation of the helices and the binding of the adamantane inhibitor to the structure (Cady et al. 2010). The homo-oligomeric state of the molecule, however, is confirmed from intermolecular NOEs in the structure (Schnell and Chou 2008). Conversely, the RDC dataset for PLN is similar to the RDC dataset of a monomeric PLN (Shi et al. 2011), suggesting that the tensor $R_h = 0.33$ might arise from the monomeric form of PLN instead of the homopentamer.

RDCs from ligands bound to homo-oligomers presents another set of examples. In these systems, the homo-oligomer has 'n' identical binding sites, and partial alignment data from the ligand should follow the symmetry of the homo-oligomeric protein.

The acyl carrier protein (ACP) binds to 1 of 3 identical sites in the UDP-N-acetylglucosamine acyltransferase (LpxA) homotrimer (Jain et al. 2004). LpxA has a C_3 axis of symmetry, and the alignment tensor of ACP bound to LpxA has an $R_h = 0.093$, which the authors argue is close to zero.

In another example, the orientation of a ligand, α-methylmannose (AMM), to a homotrimeric protein binding partner, mannose binding protein (MBP), was inferred from the alignment tensor for the RDCs of AMM bound to MBP (Bolon et al. 1999; Al-Hashimi et al. 2000). MBP has a threefold rotational symmetry axis with three AMM binding sites. In these studies, 5 or 7 RDCs were measured from AMM, and only 5 RDCs are required to fit the Saupe alignment tensor. Though the interaction of AMM with MBP may be highly specific, the interaction of MBP with the liquid crystal, aligned bicelles in this case, may not. The first study measured $R_h = 0.16 \pm 0.11$. The second study refined a series of alignment tensor solutions with R_h values in the range of *ca.* 0.03–0.33, with $R_h = 0.08$ as the most probable solution.

The analysis of ligand alignment presents its own challenges. In the case of weak binding, the ligand's alignment tensor may represent an average between bound and unbound states. In the case of strong binding to only a subset of sites, the ligand may break the symmetry of its homo-oligomeric binding partner. If an excess of ligand is used to avoid this problem, resonances from bound and unbound forms of the ligand may not be distinguishable, further complicating the analysis of the ligand's alignment tensor.

Orientation of the alignment tensor

The SVD of an RDC dataset yields the alignment tensor components, D_a and R_h, and the orientation of the molecule with respect to the *average* alignment frame. This orientation can be used to infer the axis of symmetry (Jain et al. 2004; Reardon et al. 2014), but it also may not be reliable for this purpose.

The first issue is that the angles may not be unique. A unique axis for the principal component may be selected for a completely axially symmetric alignment tensor. For an axially asymmetric alignment tensor, there are at least 4 degenerate sets of Euler angles that are solutions for the orientation of the alignment frame (Hus et al. 2008). The challenge is to select the meaningful orientation.

The second issue is that the alignment tensor represents an average of multiple orientations. We saw an example of this phenomenon with the a homodimer. For a simple 2-site exchange, the principal component of the alignment tensor changes from the z-axis to the y-axis for jump angles

between 35.26° and 54.74°. In this case, the symmetry C_2 axis no longer points along the principal component of the tensor.

AMM binding to homotrimeric MBP is an example from the literature in which the orientation of the ligand was inferred from the alignment tensor (Bolon et al. 1999; Al-Hashimi et al. 2000). In these studies, 5 or 7 RDCs were measured from AMM, and only 5 RDCs are required to fit the Saupe alignment tensor. Their analysis of the orientation of AMM with respect to MBP deviated by *ca.* 40°, and the authors suggest multiple possibilities for this discrepancy. An additional complication may be that the averaged alignment tensor orientation may not be reliable, since it could be averaged between many different interaction orientations.

Another important example is the orientation of a membrane protein in a bicelle or nanodisc. A monomeric helix, for instance, may orient at the surface of a membrane, or it may orient with the membrane normal as a transmembrane helix. The angle of orientation is encoded in the β angle, which scales all of the RDCs and plagues the analysis with the same problems described before. If the sign of S_{LC} is known, then the approximate orientation of the helix, whether β is closer to 0° or 90°, may be inferred from the sign of the D_a. This approach is nevertheless complicated by distributions of interaction orientations. It is likely simpler to ascertain the orientation of the helix using an alternate experimental technique, such PREs (Respondek et al. 2007).

Summary

We have derived the theory for uniaxial partial alignment used in measuring RDCs and RACSs of biomolecules in liquid crystals or strained gels. The orientation of the molecule with respect to the average alignment frame can be easily determined. However, there are noteworthy pitfalls in the interpretation of the average alignment frame in terms of a single interaction orientation or an n-site hop symmetry model.

First, molecules that align with only 1 interaction orientation produce simple relationships between the molecule, its orientations with respect to the alignment frame and the D_a and R_h. For asymmetric monomeric molecules with 1 interaction orientation, the alignment tensor is axially symmetric ($R_h = 0$). The fact that axially asymmetric alignment tensors ($R_h \neq 0$) are commonly measured for monomers indicates that monomers frequently adopt multiple interaction orientations. It follows that homo-oligomeric molecules may also adopt multiple interaction orientations.

Second, the possibility of multiple interaction orientations complicates the analysis of the alignment tensor components for homo-oligomeric molecules. It is possible for homo-oligomers with 3 or more subunits to produce an axially asymmetric alignment tensor—i.e. $R_h \neq 0$. This is the case when different interaction orientations change the orientation of the symmetry axis with respect to the alignment frame.

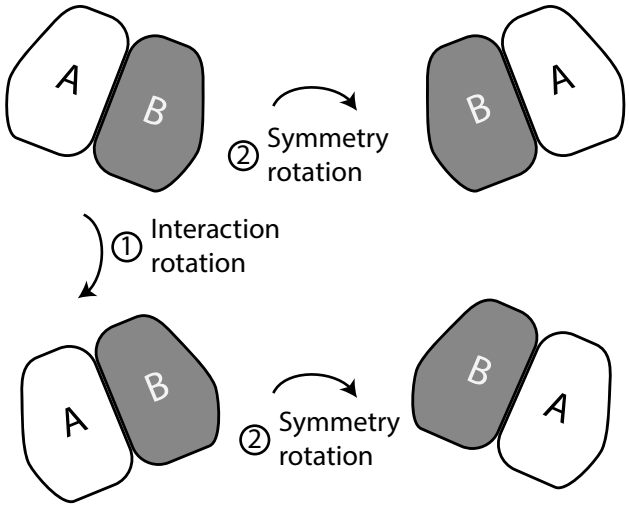

Fig. 9 Diagram demonstrating the correct order of rotations with the interaction rotation first and the symmetry rotation second. Reversing the order of rotation requires a clockwise symmetry rotation in one case and a counter-clockwise symmetry rotation in the other

Third, the Euler angles determined from an SVD analysis of RDCs or RACSs represent the molecule's orientation with respect to the average alignment frame. Consequently, the alignment tensor orientation may not accurately report on the orientation of the symmetry axis for homo-oligomers.

In summary, the alignment tensors for homo-oligomers may or may not be consistent with simple models of alignment with 1 interaction orientation. A careful analysis should confirm the number of subunits in a homo-oligomer with additional evidence, such as size-exclusion chromatography, native polyacrylamide gel electrophoresis or AUC.

Methods

Simulations

To properly account for both *interaction* orientations and *symmetry* orientations, equation (24) must be rotated first to the interaction orientation then rotated to the appropriate symmetry orientation (Fig. 9). Reversing the order of rotation requires the redefinition of the interaction rotation for each symmetric orientation.

In producing a motionally averaged set of RDCs, the normalized internuclear vector ($\mathbf{v_i}$) for each bond 'i' was calculated from a molecular structure. In our simulations, we calculated ^{1}H–^{15}N RDCs for backbone amides in the ubiquitin structure (PDB: 2MJB) (Maltsev et al. 2014).

Active rotations with a fixed coordinate system were used in the simulations. The bond vectors were first rotated to the different interaction orientations using a α' rotation about the z-axis, and a β' rotation about the y-axis and a γ' rotation about the z-axis. Thereafter the symmetric rotations were conducted by an α rotation about the z-axis and a β rotation about the y-axis.

$$\mathbf{v_i}' = \mathbf{R_y}(\beta)\mathbf{R_z}(\alpha)\mathbf{R_z}(\gamma')\mathbf{R_y}(\beta')\mathbf{R_z}(\alpha')\mathbf{v_i} \tag{33}$$

The RDC, D_i, was calculated from the z-component, z_i', of the rotated vector, $\mathbf{v_i}'$ (Losonczi et al. 1999). The initial vector, $\mathbf{v_i}$, was normalized.

$$\begin{aligned} D_i &= D_a\left\langle \tfrac{1}{2}(3\cos^2\theta_i - 1)\right\rangle \\ &= D_a\left\langle \tfrac{1}{2}(3z_i'^2 - 1)\right\rangle \end{aligned} \tag{34}$$

We used a D_a value of 10 Hz for the simulations in this study.

This transformation represents the average orientation(s) between the dipolar PAS and the laboratory frame.

The contribution of 'm' interaction orientations and 'n' symmetry orientations are average with populations p_{mn} for each.

$$\left\langle \mathbf{v_i}' \right\rangle = \left\langle \sum_{m,n} p_{m,n}\mathbf{R_y}(\beta_n)\mathbf{R_z}(\alpha_n)\mathbf{R_z}(\gamma_m')\mathbf{R_y}(\beta_m')\mathbf{R_z}(\alpha_m')\mathbf{v_i} \right\rangle \tag{35}$$

The motionally averaged vector is reintegrated in equation (34) to calculate the motionally averaged RDC.

In all cases in this manuscript, the populations are equal for the total of 'N' interaction and symmetry orientations such that $p_{mn} = N^{-1}$.

Thereafter, an SVD was calculated for the generated set of D_i RDCs with the molecular structure, using mollib (Lorieau 2017). The SVD yields the alignment tensor orientation, principal component and rhombicity. The source code for an example simulation from Fig. 7 is presented in the Supplementary Information.

Acknowledgements This work was supported by the National Science Foundation under Grant No. MCB1651598 and funds from the Department of Chemistry at the University of Illinois at Chicago.

References

Al-Hashimi HM, Bolon PJ, Prestegard JH (2000) Molecular symmetry as an aid to geometry determination in ligand protein complexes. J Magn Reson 142(1):153–158. https://doi.org/10.1006/jmre.1999.1937

Batchelder L, Niu C, Torchia D (1983) Methyl reorientation in polycrystalline amino acids and peptides: a deuteron NMR spin-lattice relaxation study. J Am Chem Soc 105(9):2228–2231. https://doi.org/10.1021/ja00346a021

Bax A (2003) Weak alignment offers new NMR opportunities to study protein structure and dynamics. Protein Sci 12:1–16. https://doi.org/10.1110/ps.0233303.Protein

Bax A, Kontaxis G, Tjandra N (2001) Dipolar couplings in macromolecular structure determination. Methods Enzymol 339(1997):127–174

Blackledge M (2005) Recent progress in the study of biomolecular structure and dynamics in solution from residual dipolar couplings. Prog NMR Spectrosc 46(1):23–61. https://doi.org/10.1016/j.pnmrs.2004.11.002

Bolon PJ, Al-Hashimi HM, Prestegard JH (1999) Residual dipolar coupling derived orientational constraints on ligand geometry in a 53 kDa protein-ligand complex. J Mol Biol 293(1):107–115. https://doi.org/10.1006/jmbi.1999.3133

Cady SD, Schmidt-Rohr K, Wang J, Soto CS, Degrado WF, Hong M (2010) Structure of the amantadine binding site of influenza M2 proton channels in lipid bilayers. Nature 463(7281):689–692. https://doi.org/10.1038/nature08722

Clore GM, Garrett DS (1999) R-factor, free R, and complete cross-validation for dipolar coupling refinement of NMR structures. J Am Chem Soc 121(39):9008–9012. https://doi.org/10.1021/ja991789k

Cornilescu G, Bax A (2000) Measurement of proton, nitrogen, and carbonyl chemical shielding anisotropies in a protein dissolved in a dilute liquid crystalline phase. J Am Chem Soc 122(41):10143–10154. https://doi.org/10.1021/ja0016194

Cornilescu G, Marquardt JL, Ottiger M, Bax A (1998) Validation of protein structure from anisotropic carbonyl chemical shifts in a dilute liquid crystalline phase. J Am Chem Soc 120(27):6836–6837. https://doi.org/10.1021/ja9812610

Dong RY (1997) Nuclear magnetic resonance of liquid crystals. Partially ordered systems. Springer, New York. https://doi.org/10.1007/978-1-4612-1954-5

Goldman M (1988) Quantum description of high-resolution NMR in liquids. Oxford University Press, Oxford

Hansen MR, Mueller L, Pardi A (1998) Tunable alignment of macromolecules by filamentous phage yields dipolar coupling interactions. Nat Struct Biol 5(12):1065–1074. https://doi.org/10.1038/4176

Jain NU, Wyckoff TJ, Raetz CR, Prestegard JH (2004) Rapid analysis of large protein-protein complexes using NMR-derived orientational constraints: the 95 kDa complex of LpxA with acyl carrier protein. J Mol Biol 343(5):1379–1389. https://doi.org/10.1016/j.jmb.2004.08.103

Jc Hus, Salmon L, Bouvignies G, Lotze J, Blackledge M, Brüschweiler R (2008) 16-fold degeneracy of peptide plane orientations from residual dipolar couplings: analytical treatment and implications for protein structure determination. J Am Chem Soc 130(47):15927–15937. https://doi.org/10.1021/ja804274s

Keniry MA, Rothgeb TM, Smith RL, Gutowsky HS, Oldfield E (1983) Nuclear magnetic resonance studies of amino acids and proteins. Side-chain mobility of methionine in the crystalline amino acid and in crystalline sperm whale (*Physeter catodon*) myoglobin. Biochemistry 22(8):1917–1926. https://doi.org/10.1021/bi00277a028

Lorieau JL (2017) Mollib: a molecular and NMR data analysis software. J Biomol NMR 69(2):69–80. https://doi.org/10.1007/s10858-017-0142-5

Lorieau J, Yao L, Bax A (2008) Liquid crystalline phase of G-tetrad DNA for NMR study of detergent-solubilized proteins. J Am Chem Soc 130(24):7536–7537. https://doi.org/10.1021/ja801729f

Losonczi JA, Andrec M, Fischer MW, Prestegard JH (1999) Order matrix analysis of residual dipolar couplings using singular value decomposition. J Magn Reson 138(2):334–42. https://doi.org/10.1006/jmre.1999.1754

Mack JW, Torchia DA (1991) A deuteron NMR study of the molecular dynamics of solid cyclopentane. J Phys Chem 95(11):4207–4213. https://doi.org/10.1021/j100164a009

Maltsev AS, Grishaev A, Roche J, Zasloff M, Bax A (2014) Improved cross validation of a static ubiquitin structure derived from high precision residual dipolar couplings measured in a drug-based liquid crystalline phase. J Am Chem Soc 136(10):3752–5. https://doi.org/10.1021/ja4132642

Oxenoid K, Chou JJ (2005) The structure of phospholamban pentamer reveals a channel-like architecture in membranes. Proc Natl Acad Sci USA 102(31):10870–10875. https://doi.org/10.1073/pnas.0504920102

Reardon PN, Sage H, Dennison SM, Martin JW, Donald BR, Alam SM, Haynes BF, Spicer LD (2014) Structure of an HIV-1-neutralizing antibody target, the lipid-bound gp41 envelope membrane proximal region trimer. Proc Natl Acad Sci 111(4):1391–1396. https://doi.org/10.1073/pnas.1309842111

Respondek M, Madl T, Göbl C, Golser R, Zangger K (2007) Mapping the orientation of helices in micelle-bound peptides by paramagnetic relaxation waves. J Am Chem Soc 129(16):5228–34. https://doi.org/10.1021/ja069004f

Rose ME (1957) Elementary theory of angular momentum. Dover Publications Inc., New York. https://doi.org/10.1007/BF02860403

Sarkar S, Young P, Torchia D (1986) Ring dynamics of DL-proline and DL-proline hydrochloride in the solid state: a deuterium nuclear magnetic resonance study. J Am Chem Soc 108:6459–6464. https://doi.org/10.1021/ja00281a002

Saupe A (1968) Recent results in the field of liquid crystals. Angew Chem Int Ed Engl 7(2):97–112. https://doi.org/10.1002/anie.196800971

Schmidt-Rohr K, Spiess H (1994) Multidimensional solid-state NMR and polymers. Academic Press Inc., San Diego, CA

Schnell JR, Chou JJ (2008) Structure and mechanism of the M2 proton channel of influenza A virus. Nature 451(7178):591–595. https://doi.org/10.1038/nature06531

Shi L, Traaseth NJ, Verardi R, Gustavsson M, Gao J, Veglia G (2011) Paramagnetic-based NMR restraints lift residual dipolar coupling degeneracy in multidomain detergent-solubilized membrane proteins. J Am Chem Soc 133(7):2232–2241. https://doi.org/10.1021/ja109080t

Steigel A, Spiess HW (1978) Dynamic NMR spectroscopy. Springer, New York

Tjandra N, Bax A (1997) Direct measurement of distances and angles in biomolecules by NMR in a dilute liquid crystalline medium. Science 278(5340):1111–1114. https://doi.org/10.1126/science.278.5340.1111

Tolman JR, Flanagan JM, Ma Kennedy, Prestegard JH (1995) Nuclear magnetic dipole interactions in field-oriented proteins: information for structure determination in solution. Proc Natl Acad Sci USA 92(20):9279–9283

Torchia DA (1984) Solid state NMR internal dynamics !. PoLAR 21:125–144

Torchia DA (2015) NMR studies of dynamic biomolecular conformational ensembles. Prog Nucl Magn Reson Spectrosc 84–85:14–32. https://doi.org/10.1016/j.pnmrs.2014.11.001

Tycko R, Blanco F, Ishii Y (2000) Alignment of biopolymers in strained gels: a new way to create detectable dipole–dipole couplings in high-resolution biomolecular NMR. J Am Chem Soc 122(17):9340–9341. https://doi.org/10.1021/ja002133q

Zweckstetter M, Bax A (2000) Prediction of sterically induced alignment in a dilute liquid crystalline phase: aid to protein structure determination by NMR [11]. J Am Chem Soc 122(15):3791–3792. https://doi.org/10.1021/ja0000908

Zweckstetter M, Hummer G, Bax A (2004) Prediction of charge-induced molecular alignment of biomolecules dissolved in dilute liquid-crystalline phases. Biophys J 86(6):3444–3460. https://doi.org/10.1529/biophysj.103.035790